RAE2026

The Creation of an Inlay-Knitted Buoyant Fabric

Prof. Chupo HO

UoA38

11.2025

Contents

The Creation of an Inlay-Knitted Buoyant Fabric

Descriptor

Foam blocks have been widely used as the primary means of creating buoyancy in swimwear. However, discomfort may arise owing to differences in fit and a lack of mobility. Swimwear that includes foam blocks tends to be bulky because of uneven buoyancy distribution. The wearer's movement is inhibited, and the shifting of the swimwear during activity is problematic.

Through the application of the inlay knitting concept, the research team successfully developed a 'knitted' buoyant fabric. Owing to its high flexibility and bendable properties, this buoyant fabric can reduce bulkiness, and the bendability of its knitted structure can enhance mobility when applied to swimwear design. The knitted buoyant fabric can be layered in the swimwear, allowing for adjustment of the buoyancy. More than 30 samples were developed during the study, featuring different knitting structures, fiber types and buoyant media. The best combination for further application was identified based on testing results and objective data analysis.

The publications from this study explain the development of the knitted buoyant fabric and cover critical information, including the selection of buoyant materials, yarns and knitted structures. The correlations of these components were studied and analysed by calculating the net buoyancy (Archimedes' principle) and performing a statistical analysis (multivariate analysis of variance [MANOVA] and multiple linear regression). The research data suggest a two-stage approach to create the optimal combination for creating a knitted buoyant fabric for swimwear.

The research process for the knitted buoyant fabric was documented in three peer-reviewed papers. The creative method of knitting explored a new direction in the development of swimwear and related water sports products. The data and production details can be used as benchmarks for further improvements of knitted buoyant fabrics by future research teams. As a team leader, Prof. Ho's responsibilities included research design, methodological development and data evaluation. (300 words)

Personal Profile: Prof. Chupo HO

Associate Professor Chu-po Ho is a researcher specialising in the design of functional sports apparel/textile and the development of related equipment. His research focuses on the integration of cutting-edge knitting technologies, the ergonomic design of sports clothing to enhance performance, and the creation of innovative 3D-printed structures through modifications of knitting loop stitch mechanisms.

As Principal Investigator (PI), Professor Ho has submitted three MCOs. In MCO1, he led a team in creating a flexible buoyant fabric using a modified inlay knitting technique. This fabric is notable for its flexibility and bendable qualities, which significantly reduce the bulk of conventional swimming devices. In MCO2, he advanced the application of this buoyant fabric in designing a range of buoyant swimming vests for children. The design features adjustable buoyancy to accommodate varying swimming abilities among children. The development stages of the vests and their ratings in wearer trials were also reported. MCO3 was a collaborative project funded by the School of Fashion and Textiles and the Research Institute of Sports at The Hong Kong Polytechnic University, amounting to HKD 700,000. In this initiative, Professor Ho directed another team in developing experimental 3D-printed lattice-structured materials inspired by the high compression properties of knitted spacer fabrics. This design was applied to bicycle saddles, which are crucial for enhancing rider comfort and performance, in accordance with the requirements of the funding scheme.

In addition to his research publications, patents and design registrations, Professor Ho has received international recognition for his work, including the 2024 Red Dot Design Award (winner in Design Concept) and the Gold Award at the 2022 Inventions Geneva Evaluation Days.

Research Questions

1. What are the drawbacks of using foam blocks in conventional buoyant swimwear design?

2. What is inlay knitting technology, and how can it be applied in creative textiles?

3. How can inlay knitting be used to insert buoyant material into knitted structures?

4. What criteria and data regarding inlaid buoyant materials (e.g. inner and outer diameters, linear density and wall thickness) can influence the performance of an inlay knitted fabric?

5. How do buoyant materials, knitting structures and yarns correlate in creating knitted buoyant fabrics?

Research Outputs

1. Practice-based artefacts
2. Academic publications × 2
3. Exhibition poster × 1

Research Outputs

This study created 30 novel knitted buoyant fabrics using a combination of different knitting structures, yarns and inlay foam materials (Figure 1). After evaluating a combination of various objective measurements and analysing the data using SPSS, the best combination that balances buoyancy with tensile strength and compression performance was identified. Compared with traditional foam blocks, the knitted buoyant fabric 'inlays' the foam tube, allowing the features of knitted fabric (flexibility and high bendability) to be potentially utilised in the creation of garments for watersports when used as a buoyant medium (Figure 2). Figure 16 shows the fabric samples (EPEnH2 and EPE2).

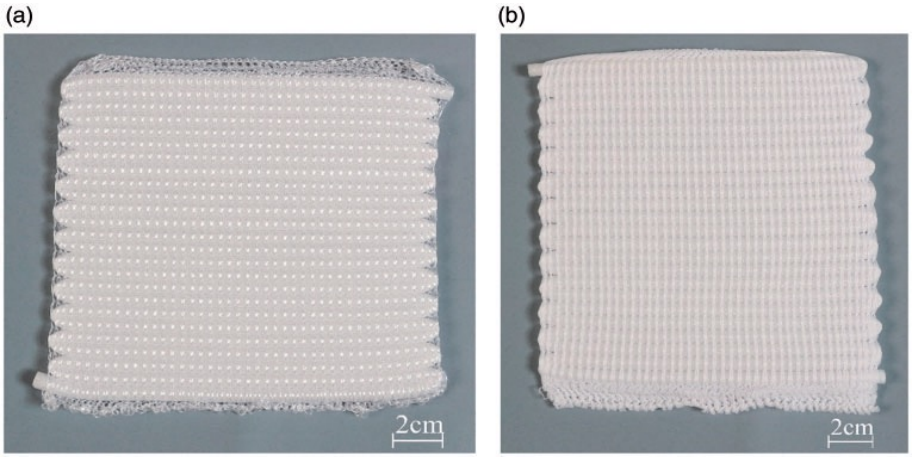

Figure 1. Front view of the inlaid knitted fabric: (a) EPEnH2 and (b) EPE2

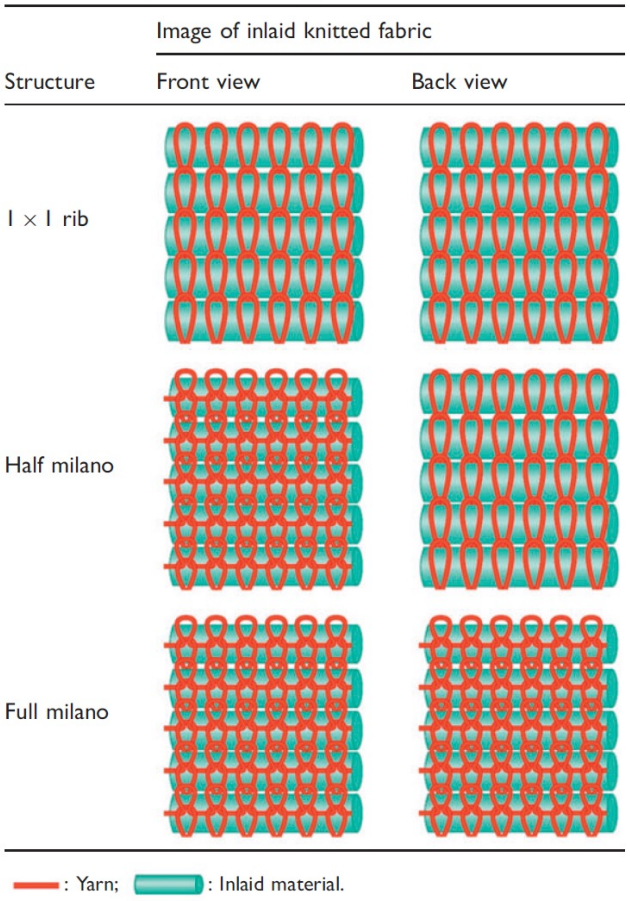

Figure 2. Drawings of buoyant fabrics knitted using the inlay method

Research Outcomes

The prototypes of the knitted buoyant fabric are shown in the following figures. Figure 3 shows the shape retention property of the knitted buoyant fabric and its bendable property that enables the wearer to move freely.

Figure 4 shows the experiment of joining together different knitted buoyant fabrics. The length of the inlay foam tube created aesthetic attractiveness to the swimsuit design.

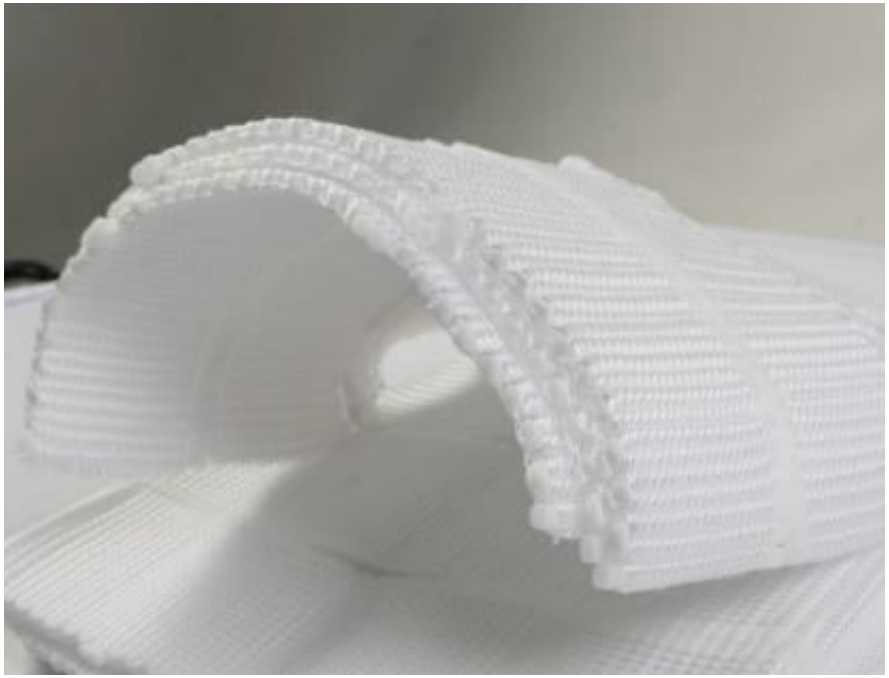

Figure 3. Shape retention property of the inlaid knitted fabric

.

Figure 4. Joining panels of the knitted buoyant fabric

Research Field and Key References

1. What are the problems of the current foam blocks applied in buoyant swimwear?

In recent decades, foam blocks have been used as the main component to provide buoyancy in swimwear. Swimwear with foam blocks are extremely bulky owing to a lack of buoyancy distribution. The wearer's movement is inhibited, and the shifting of the swimwear during wear is problematic (U.S. Patent No. 15/303739, 2017). Moreover, as buoyancy increases when the buoyant swimwear is worn, the wearer may find reduced ability to swim horizontally underwater (Gagnon et al., 2012). Finally, it is inconvenient to doff the entire suit when using the toilet or making a diaper change (U.S. Patent No. 7,438,619, 2008). As a result, children are often reluctant to wear bulky, aesthetically unpleasing and uncomfortable buoyant devices or swimwear (U.S. Patent No. 6,112,327, 2000).

2. What is inlay in knitwear technology?

By using inlay knitting, it is possible to create a buoyant fabric using a knitting machine, as the coarse inlaid materials that cannot usually be knitted into the intermeshed loops can be incorporated into the structure during the same knitting cycle. The inlaid knitted structure has been widely used to create different textile designs. For example, Jennifer Barrett, a UK designer, uses inlay knitting in her knitwear design by contrasting traditional techniques, such as knot making, with unconventional materials to explore architectural forms and optical illusions.

[Image]

Image not included. Please contact the author for permission to view or reuse.

Figure 5. Inlaid knitted structure in (a) a cardigan and (b) pullover by Jennifer Barrett. adapted from 'Knot knitting' by J. Barrett, 2015. Retrieved from https://www.artsthread.com/portfolios/knotknitting/. Copyright 2015 by Arts Thread Limited.

Research Methods, Prototypes and Material

1. **Calculation of net buoyant force**: Following Archimedes' principle, the net buoyant force of the samples is calculated as follows (Picelli et al., 2017): Fnet = ρf Vf g − mg
2. **Measuring the volume of buoyant fabric samples** (Figure 6)
3. The buoyant force was corrected to the values of the standard temperature and pressure conditions using the equation (BCl = Bl × Pl101.3 × 293.15 Tl + 273.15), and the specific buoyancy of each fabric sample was calculated using the equation (SBl = BClV) in accordance with the standard ISO 12402-7:2006 (ISO, 2006a).
4. **Compression** and **tensile strength** properties

Statistical Analysis

Multiple linear regression and MANOVA were used on the buoyant fabric samples to examine the mean differences between the three independent variables (inlaid material, yarn and knitted structure) on the three dependent variables (net buoyant force, compression and tensile properties).

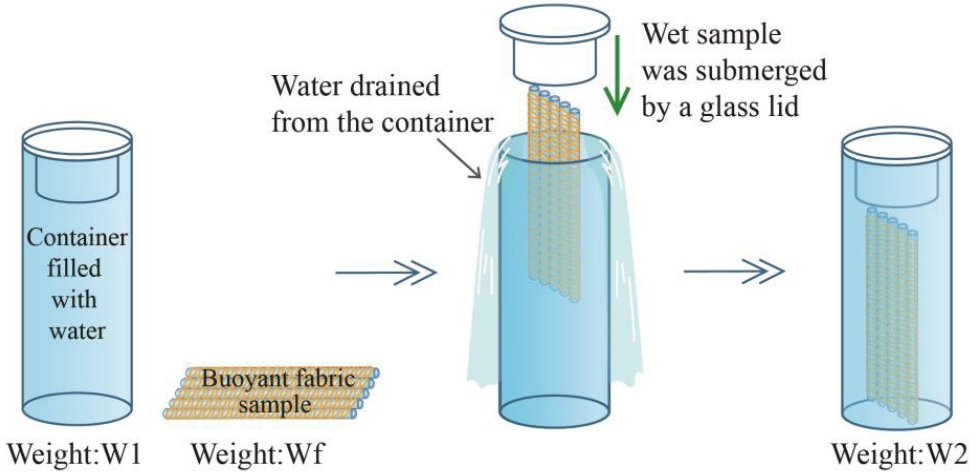

Figure 6. Measuring the volume of buoyant fabric samples

Research Methods, Prototypes and Material

The development of the inlaid knitted fabric comprised two stages:

Stage 1: Selection of the inlaid buoyant material (Figures 7 and 8)

Stage 2: Selection of the knitted structure and yarn

To provide the swimwear with optimal buoyancy and the least amount of bulkiness, the specific buoyancy was calculated to investigate the ability of each sample with the same volume to provide buoyancy.

The fabric samples with the highest specific buoyancy were selected for the development of the swimwear. The compression and tensile properties were also measured and compared. The influence of the inlaid material, knitted structure and yarn on the net buoyant force and mechanical properties are discussed.

Figure 7. Prototype example: Knitted fabric inlaid with buoyant tube material 1.

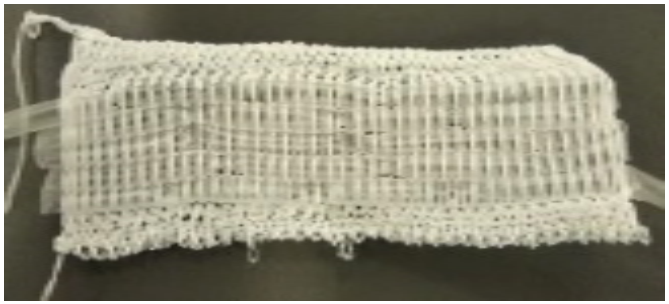

Figure 8. Prototype sample: Knitted fabric inlaid with buoyant tube material 2.

Research

Stage I: Selection of the Inlaid Buoyant Material

Three tube materials with different diameters were sourced, including one made of polyethylene (PE), which is already used in life jackets for its buoyancy potential in textile materials (Kalayci et al., 2015). As the inlaid tubes must be light in weight, floatable, flexible and soft enough for laying in during the knitting process, PE, polyvinyl chloride (PVC) and silicone are chosen as materials. As PE varies widely in density, hardness, thickness and other physical and mechanical properties, it has diverse applications ranging from plastic bags and bottles to gas pipes with biodegradable properties (Cole-Hamilton, 2010). PVC is a thermoplastic material that becomes soft and flexible when heated and retains a fixed configuration when cooled, depending on the amount and type(s) of plasticisers used (Gadler, 2014) (Figure 9 and Table 1).

Low density and air trapped between fibres are the key buoyancy characteristics of polypropylene (PP) (Cole-Hamilton, 2010; Kalayci at el., 2015). Thus, PP yarn was selected as the knitting yarn to fabricate the buoyant knitted fabric.

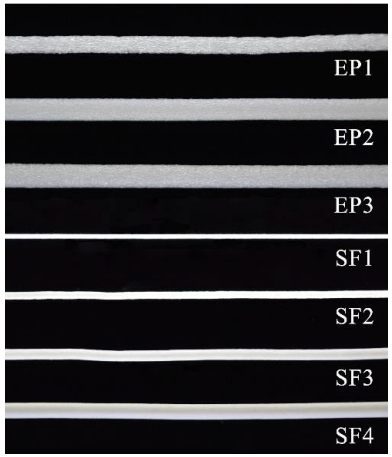

Figure 9. The inlaid materials: (a) tubes and (b) foam rods

	Tube code	Materials	Microscopic view/ image
Inlaid tube	P1–P2	PVC	
	S1–S3	Silicone	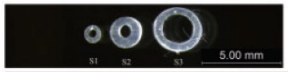
	E1–E4	Polyethylene	
Yarn		75/72d 100% Polypropylene	

Table 1. Materials used for the inlay and knitted parts

Research Material for Stage I (Selection of the Inlaid Buoyant Material)

Half Milano stitches are used to lay in the buoyant tube between the knitting loops. This stitch consists of one row of double jersey and one row of single jersey (Zhang et al, 2010; Chong et al, 2013). Its construction creates space between the loops in the front and back needle beds, enabling the filament to be laid in during knitting (Figure 10).

All samples were prepared under the same knitting tension and parameters, with a dimension of 38 courses that included 25 courses of inlays in half Milano stitch and 40 wales. The length of the inlaid tube was controlled to 337.56 cm, with 2% variation. Table 6 describes the knitting notation and symbols, and represent the double- and single-knit stitch, respectively. Finally, both ends of the inlaid tube are blocked by heat fusion.

Sample code	Inlaid tube	Fabric weight (g/m^2)	Thickness (mm)	Wale density (loops/cm)	Course density (loops/cm)
PV1	P1	708.94	2.42	3.04	4.51
PV2	P2	1083.10	2.90	2.97	4.44
SI1	S1	346.26	1.50	2.99	4.80
SI2	S2	1023.75	2.38	2.96	4.69
SI3	S3	1299.11	3.15	2.95	4.16
PE1	E1	315.15	2.31	3.13	4.97
PE2	E2	412.23	2.90	2.90	4.29
PE3	E3	511.04	4.29	2.91	3.84
PE4	E4	720.29	6.54	2.87	4.06
C	Nil	101.56	0.80	4.10	4.32

Table 2. Specification of the inlaid knitted specimens with different inlaid materials and control fabric

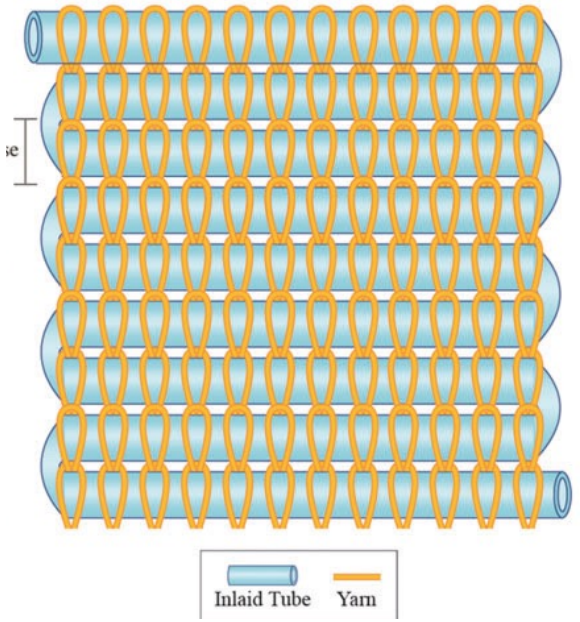

Figure 10. Inlaid knitted fabric sample

Research Method

Measurement for Stage I (Selection of the Inlaid Buoyant Material)

Measurement

To study the relationships between the buoyant force of the inlaid fabrics and linear density, the inner and outer diameters of the inlaid plastic tubes, and the volume of the fabric sample were measured in accordance with Archimedes' principle. The fabric sample was placed in a water-filled vessel, where its volume was calculated on the basis of the volume of water displaced. As the buoyant tubes used in this study were highly compressible, a non-contact approach was adopted. The cross-section of the buoyant tubes was initially imaged with a Leica M165C stereo microscope, and the inner and outer diameters of the buoyant tubes were subsequently measured in four directions (Figure 11). According to Archimedes' principle, a substance submerged in a liquid displaces a volume of liquid equal to its volume (Kiriktas et al, 2018). Thus, the volume of the fabric specimen was calculated by estimating the difference between the initial weight and the weight of the remaining water after the insertion of the fabric. Five specimens were knitted for each fabric type, and each specimen was tested three times. The mean value obtained from 15 tests was used, and the images of the inlaid knitted fabrics PE3 and PE4 are shown in Figure 12.

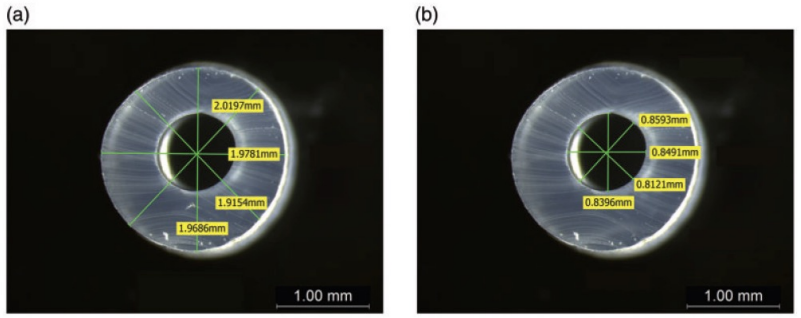

Figure 11. Microscopic view of the S2 tube measuring (a) the outer and (b) inner diameters

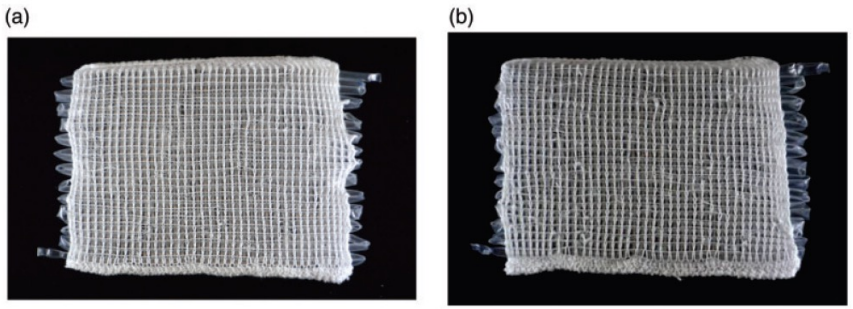

Figure 12. Front view images of the inlaid knitted fabrics (a) PE3 and (b) PE4

Research Method for Stage I

Fabric Density and Buoyant Force

The key finding of this study is that the inner diameter, outer diameter and linear density of the inlaid tube and their interactions significantly affected the buoyancy performance of the inlaid knitted fabric. A higher net buoyant force means that the fabric is more buoyant. Figure 13 shows the schematic of the forces exerted on a buoyant knitted fabric. The experimental and multiple regression analysis results are presented in Table 3.

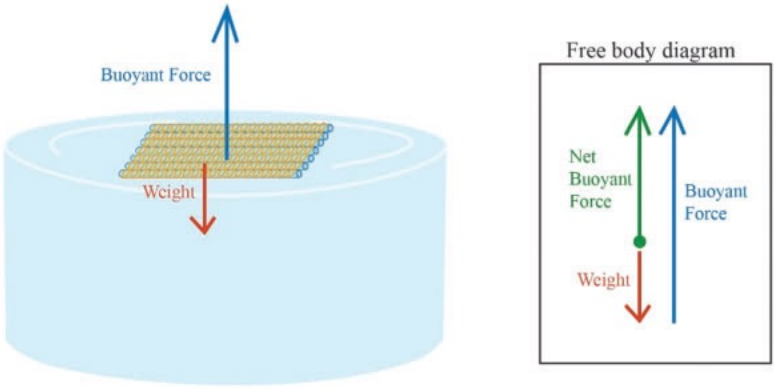

Figure 13. Schematic of the forces exerted on the buoyant knitted fabric

Table 3. Results of the multiple regression analysis for identifying the predictors of the net buoyant force

Properties	Factor	R	R^2	B	t	P	F	P
Net buoyant force[c]	Inner diameter[a]	0.78	0.60	−2.39	−7.41	<.001	200.58	<.001
	Outer diameter[b]	0.82	0.67	1.73	4.90	<.001	135.67	<.001
	Linear density	0.83	0.69	−0.22	−2.28	<.030	95.05	<.001

Note: All coefficients are rounded to the nearest two decimals.
[a]Square root of inner diameter.
[b]Square root of outer diameter.
[c]Inverse of net buoyant force.

Research Method for Stage I

Multiple Linear Regression Analysis

The data from the experiment were analysed using SPSS 23. Multiple linear regression analysis was used to examine the relationships between the dependent variable (the net buoyant force of the inlaid knitted fabric) and the following three independent variables:

(1) inner diameter of the inlaid tube

(2) outer diameter of the inlaid tube

(3) linear density of the inlaid tube

The significance level of the statistical analysis was set at 0.05. Histograms, Q–Q plots and the measures of skewness and kurtosis indicate that the distributions of the net buoyant force, inner diameter and outer diameter were significantly left-skewed. Hence, a square root transformation was conducted on the inner and outer diameters. Inverse transformation was performed on the net buoyant force because of the positive skewness. Evaluation of the newly transformed distributions indicates that they were close to a normal curve.

Fabric code	Inner diameter (mm)	Outer diameter (mm)	Wall thickness (mm)	Linear density (g/cm)	Total gas volume of fabric (cm^3)	Net buoyant force (N)
PV1	1.17	1.86	0.70	0.02	3.58	0.03
PV2	1.64	2.46	0.82	0.03	7.09	0.04
SI1	0.56	1.09	0.54	0.01	0.79	0.06
SI2	0.84	1.97	1.13	0.03	1.88	0.03
SI3	1.95	2.84	0.88	0.04	10.10	0.10
PE1	1.57	1.83	0.26	0.01	6.48	0.05
PE2	2.52	2.83	0.31	0.02	16.86	0.14
PE3	3.95	4.27	0.32	0.02	42.31	0.29
PE4	4.48	4.82	0.35	0.04	55.80	0.41
C	Nil	Nil	Nil	Nil	Nil	0.03

Table 4. Physical properties and net buoyant force of the fabrics

Research Findings for Stage I

Inner and Outer Diameters of the Inlaid Tube

The multiple linear regression analysis indicates that the inner diameter of the tube is the most important factor affecting the net buoyant force.

Consistent with the analytical results, the inner diameter of S3 in SI3 is 19%, and the total gas volume of the fabric is 43% greater than that of P2 in PV2, but the net buoyant force of SI3 is 150% higher than that of PV2.

However, the net buoyant force decreased with an increase in the inner diameter and gas volume of the fabric from SI1 to SI2. Moreover, despite its higher net buoyant force, The SI1 fabric had an inner diameter (of S1) and gas volume smaller than those of the PV1 and PV2 fabrics. To determine the reason underlying this aberrant result, the linear density of the inlaid tube was investigated, and the results are discussed in the net section.

The inner diameter of the inlaid tube affects the gas volume inside the tube, whereas the outer diameter controls the wall thickness of the tube. Therefore, the regression model predicted that the net buoyant force would increase with an increase
and decrease in the inner and outer diameters, respectively. Experimentally, the net buoyant force of the inlaid fabric increased with an increase in the outer diameter of the inlaid tubes (Figure 10b). The net buoyant force was the highest in PE4, followed by PE3. This result diverges from the predicted result of the regression model, possibly because the buoyant force is also affected by the linear density of the inlaid tube.

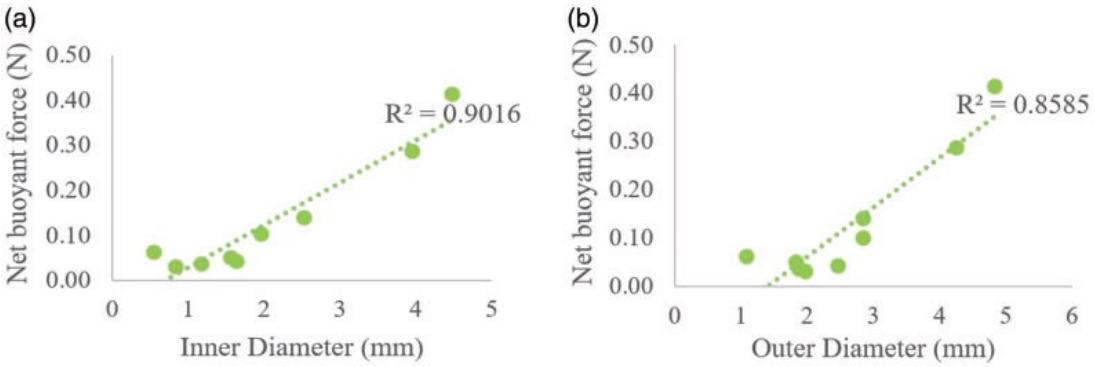

Figure 14. Comparison of the net buoyant force of inlaid fabrics with the (a) inner and (b) outer diameters of inlaid tube

Research Findings for Stage I
Linear Density of the Inlaid Tube

In general, the net buoyant force increased with an increase in linear density, which was consistent with the predicted result of the regression model (Table 4). The linear density of E2 in PE2 was similar to that of E3 in PE3 and caused a steep increase in the net buoyant force. This is because the inner diameter of E3 was 57% larger than that of E2, which means that the increase in the gas volume of the tube was disproportionately larger than the change in linear density.

Therefore, the net buoyant force of PE3 was 107% larger than that of PE2. In SI2, the linear density of S2 was triple that of S1 in SI1, but the inner diameter of S2 was only 50% larger than that of S1, and the total gas volume of SI2 is 138% higher than that of SI1. Therefore, the increase in the gas volume was much lower than the change in linear density. Moreover, the linear density is affected by the wall thickness and the type of plastic material used in the tube. As both SI1 and SI2 were made of the same silicon plastic material and thus had the same plastic density, the lower net buoyant force might be due to the wall thickness of the inlaid tube (as discussed in phase 3).

In addition, SI1 had a higher net buoyant force and a smaller linear density (of S1) than the PV1 and PV2 fabrics, consistent with the theoretical principle that a less dense object has greater buoyant ability (Nelson et al, 2010). Therefore, the SI1 fabric had a higher net buoyant force than the PV1 and PV2 fabrics. However, this result diverged from the result predicted by the multiple linear regression. To investigate the reason why SI2, PV1 and PV2 has lower net buoyant forces than SI1, the effect of the wall thickness of the inlaid tube on the buoyant force of the fabric is also investigated in the net section.

Research Findings for Stage I
Wall Thickness of the Inlaid Tube

The regression model indicates that the net buoyant force of the fabric was mostly affected by both the inner and outer diameters, in turn affecting the wall thickness of the inlaid tube. Consistent with the expectation that the wall thickness would remain constant regardless of the diameter of the inlaid tube, the gas volume increased with the increase in the outer diameter of the inlaid tube. However, the wall thickness varied even among the same type of inlaid tubes and was similar between the PE tubes of different diameters but dissimilar between the PVC and silicon tubes (Table 4).

The large decrease in the net buoyant force of SI2 was because S2 had the thickest wall thickness among the inlaid tubes. The outer diameter of S2 was 81% larger than that of S1, but the inner diameter of S2 was only 50% larger than that of S1. This makes the wall of S2 109% thicker than that of S1 (corresponding to an increase in linear density of 200%).

Compared with the inner diameter, the outer diameter of the inlaid tube showed a greater increase that caused an increase in the wall thickness and tube weight. Consequently, the net buoyant force of SI2 was lower than that of SI1. The wall thickness of S1 in SI1 was also smaller than those of the PV1 and PV2 fabrics, making its net buoyant force higher than those of the fabrics with PVC tubes.

Conclusion for Stage I

This research developed buoyant, inlaid knitted fabrics for buoyant swimsuit applications. The inner diameter, outer diameter and linear density of the inlaid tube significantly affected the net buoyant force of the fabric. The inner diameter of the inlaid tube was the strongest predictor of the net buoyant force of the fabric, followed by the outer diameter and linear density of the inlaid tube. These results indicate that the higher net buoyant force is a function of a larger inner diameter, smaller outer diameter and larger linear density of the inlaid tube. The divergence between the results for fabrics inlaid with silicon tube and the buoyant force predicted by multiple linear regression indicates that the net buoyant force is also affected by the wall thickness of the inlaid tube. The net buoyant force of the silicone tubes (SI1 and SI2) decreased with increases in the inner diameter and gas volume. The large decrease in the net buoyant force of SI2 can be attributed to the thickest wall thickness of the inlaid tube (S2).

Moreover, the smaller wall thickness of S1 in SI1 provided evidence of higher net buoyant force with a smaller inner diameter and linear density than those of the fabrics with PVC tubes. By taking advantage of the flexible silicone, more gas can be stored at the corner of the tube at the fabric's edges, which implies that silicone performs better than PVC. In future research, knitted fabrics made using different types of stitch should be investigated to establish the relationship between knitting stitches, buoyancy and the mechanical properties of buoyant knitted fabrics.

Research Material

Stage II – Correlation Between Knitted Structure, Yarns and Inlaid Foam Tubes

Although the application of inlaid knitted fabric has been examined in some studies, little research has been conducted on the relationships between the inlaid material, yarn and knitted structure and buoyancy performance or the mechanical properties of inlaid knitted buoyant fabric. In this study, the effects of the inlaid material, yarn and knitted structure on the net buoyant force, compression and tensile properties of inlaid knitted fabrics were investigated. To facilitate an efficient data collection process, a design of experiments (DOE) table was used (Table 5). The details of the inlaid materials and knitting yarns are presented in Table 6. The findings of this study provide a better understanding of the effects of the inlaid knitted structure on the properties of buoyant fabric, which affect the fabric selection criteria when developing buoyant swimwear.

Factor	Levels				
Inlaid material	Polyvinyl chloride (PVC) tube	Silicone tube	Polyethylene (PE) tube	Expandable polyethylene (EPE) foam rod	Silicone foam rod
Yarn	Solid polypropylene	Hollow polypropylene			
Knitted structure	1 × 1 rib	Half milano	Full milano		

Table 5. Design of experiments (DOE)

Inlaid material/knitting yarn	Code	Material	Microscopic view/image
Inlaid tube	P1–P2	Polyvinyl chloride (PVC)	
	S1–S3	Silicone	
	E1–E4	Polyethylene (PE)	
Inlaid foam	EP1–EP3	Expandable polyethylene (EPE)	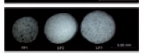
	SF1–SF4	Silicone foam	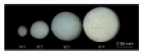
Yarn	PP	75D/72 F 100% solid polypropylene (PP)	
	HPP	250D 100% hollow polypropylene (HPP)	

Table 6. Materials used for the inlay and knitted parts

Research Material for Stage II

Three tubes and two foam rods of various diameters were sourced from the market. PE, PVC and silicone were chosen as they are buoyant, flexible and soft enough to be laid in during the knitting process. The details and cross-sections of each inlaid tube, the foam rods and the knitting yarn are illustrated in Figure 15. Owing to the advantages of the space created with a double-knitted structure, half Milano, full Milano and 1 × 1 rib were chosen as the main structures of the knitted fabric for comparison.

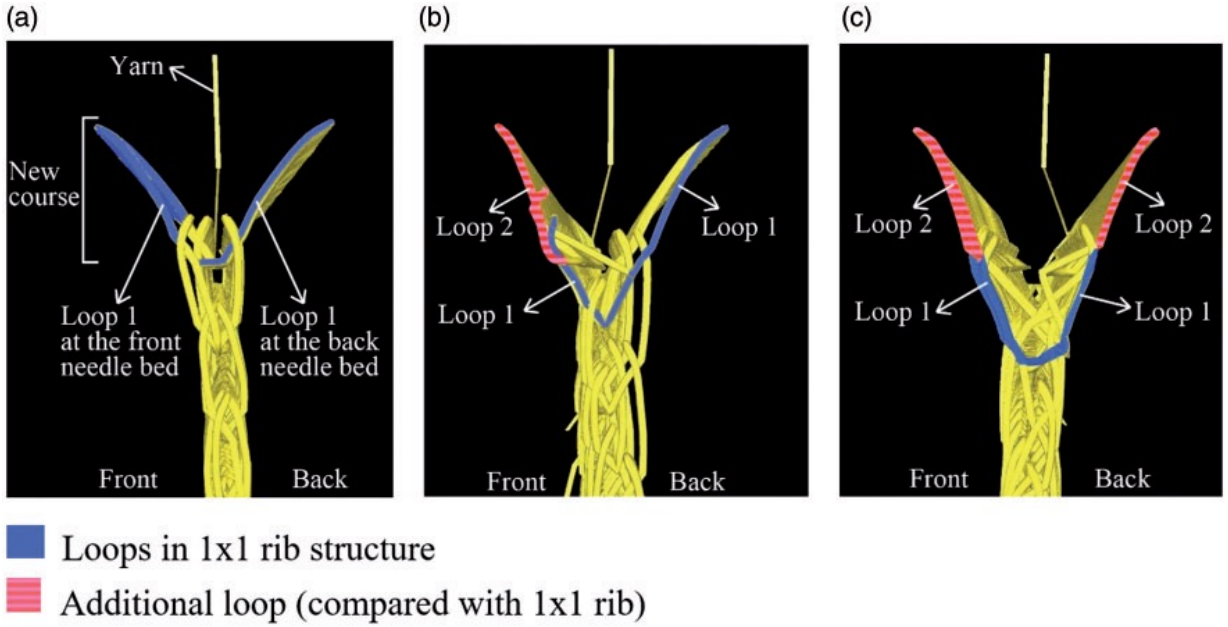

Figure 15. Side view of the knitted structure simulations of (a) 1 × 1 rib, (b) half Milano and (c) full Milano

Research Method for Stage II

With the combination of different inlay foam tubes, yarns and knitting structures, 29 knitted samples were created (including the ones without buoyant materials inserted as controlled samples), and different specimen codes were assigned to them.

To examine the relationships among the inlaid material, yarn and knitted structure on the net buoyant force, the volume of the fabric was measured, and the net buoyant force was calculated on the basis of Archimedes' principle.

This method was validated using buoyancy measurement systems with a good agreement between the calculated and measured buoyant forces. As the buoyant tubes and foam rods used in this study are highly compressible, the inner and outer diameters of the tubes and the outer diameters of rods were measured in four directions with a stereo microscope (M165C, Leica Microsystems, USA) through a non-contact approach. The fabric thickness was measured using a dial thickness gauge (Model H, Peacock Ozaki Mfg. Co., Ltd., Japan) with a measured force that was less than 1.8 N and an accuracy of 0.01 mm. According to Archimedes' principle, a substance submerged in a liquid displaces a volume of liquid equal to its volume.49,50. Thus, the volume of the fabric was calculated by measuring the volume of the displaced water.

A MANOVA was used to determine the mean differences among the levels of the three independent variables (inlaid material, yarn and knitted structure) on the three dependent variables (net buoyant force, compression and tensile properties).

Research Method for Stage II: MANOVA Results

Table 7. MANOVA Results of the Stage II Experiment

Source [h]	Properties	Dependent variable	Type III Sum of Squares	*df*	Mean Square	*F*	*Sig.*
Inlaid material [f]	Buoyancy	Net buoyant force [a]	10.17	4	2.54	64.65	0.00
	Compression	LC	0.14	4	0.03	3.36	0.01
		RC	2271.45	4	567.86	13.72	0.00
	Tensile	Maximum load (Wale direction) [b]	79.77	4	19.94	4.98	0.00
		Energy at Maximum load (Wale direction) [c]	0.32	4	0.08	4.17	0.01
		Maximum load (Course direction) [d]	810.87	4	202.72	59.09	0.00
		Energy at Maximum load (Course direction) [e]	5.92	4	1.48	57.87	0.00
Knitted structure [g]	Compression	WC	2.34	2	1.17	10.25	0.00
	Tensile	Maximum load (Wale direction) [b]	82.55	2	41.28	10.30	0.00
		Energy at Maximum load (Wale direction) [c]	0.43	2	0.21	11.25	0.00

Note: all coefficients are rounded to the last two decimals.

[a] Logarithm of net buoyant force

[b] Square root of maximum load (wale direction)

[c] Square root of energy at maximum load (wale direction)

[d] Square root of maximum load (course direction)

[e] Square root of energy at maximum load (course direction)

[f] Pillai's trace= 2.32, $F_{(df=32,\ 248)}$ =10.75, p<.001, η^2=.58

[g] Pillai's trace= .71, $F_{(df=16,120)}$ =4.13, p<.001, η^2=.36

[h] No significant difference found between yarns (Pillai's trace= .13, $F_{(df=8,\ 59)}$ =1.07, p>.05, η^2=.13)

Research Findings for Stage II

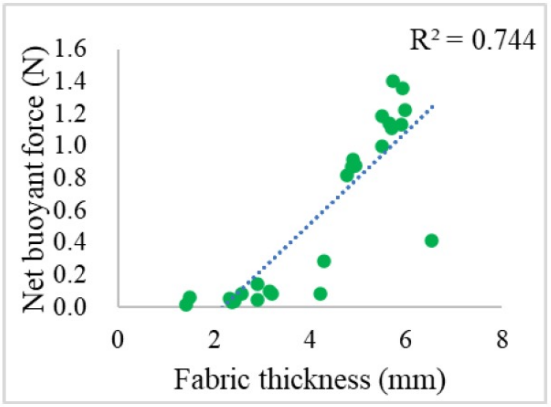

Figure 16. Comparison of the net buoyant force and thickness of the inlaid knitted fabrics

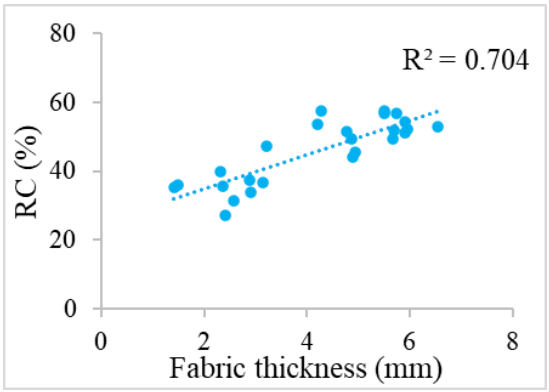

Figure 17. Comparison of the RC and thickness of the inlaid knitted fabrics

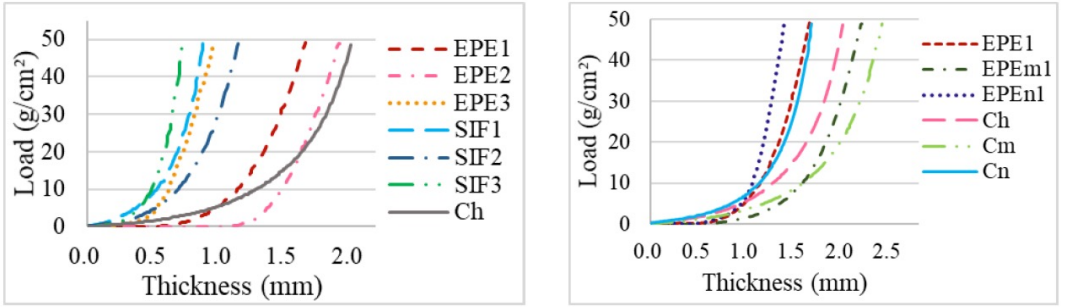

Figure 18. Compression behaviours of fabrics with various (a) inlaid materials and (b) knitted structures

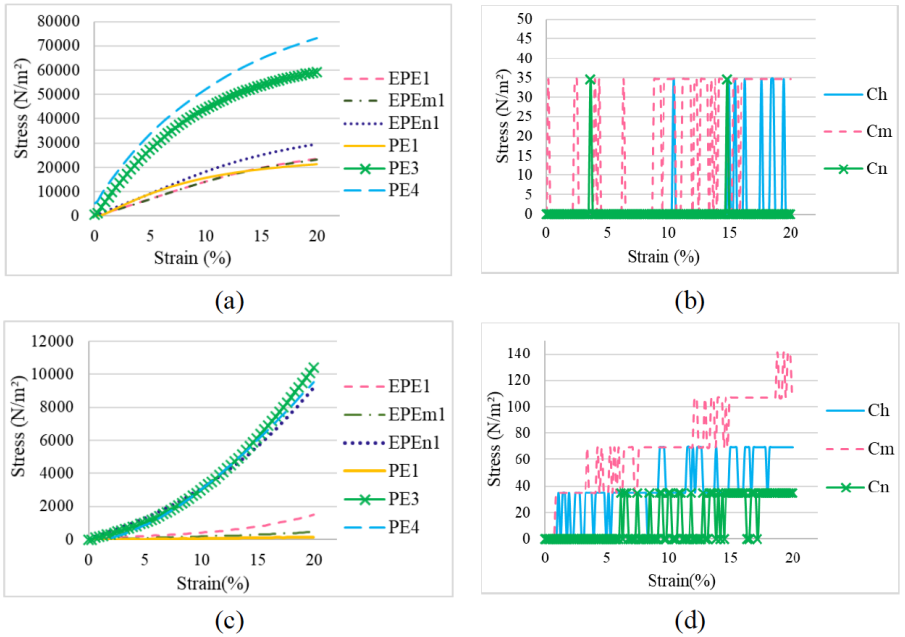

Figure 19. Stress-strain curves of the tensile properties in course direction for (a) the inlaid knitted and (b) control fabrics, and wale direction for (c) the inlaid knitted and (d) control fabrics

Research Findings for Stage II

The MANOVA results show an overall significant difference between the inlaid materials [Pillai's trace = 2.32, $F_{(32,248)}$ = 10.75, $p < .001$] and knitted structure [Pillai's trace = .71, $F_{(16,120)}$ = 4.13, $p < .001$] on the net buoyant force and mechanical properties of the fabric samples (Table 7). However, no significant difference was found between the different types of yarns [Pillai's trace = .13, $F_{(8,59)}$ = 1.07, $p > .05$). The inlaid material accounts for 58% of the variance in the overall buoyancy and mechanical properties ($\eta^2 = .581$), and the knitted structure accounts for 36% ($\eta^2 = .355$). This implies that the variances in the buoyancy and mechanical properties of the fabric samples are mainly due to inlaid material.

The inlaid material accounts for 80% of the variance in the overall buoyancy ($\eta^2 = .797$). This confirms that the net buoyant force of the fabric is mainly affected by the inlaid material. The inlaid knitted fabrics also showed a higher net buoyant force than all the control fabrics. This confirms that the additional buoyant force is provided by the inlaid material. The net buoyant force of the inlaid knitted fabrics increases with fabric thickness. As fabric thickness is mainly affected by the diameter of the inlaid material, the volume of air in the tube/rods increases with the diameter of the tube/rods, resulting in a higher net buoyant force.

Among all the fabric samples. EPEnH3 had the highest specific buoyancy, followed by EPEn3. Both EPEnH3 and EPEn3 are possible candidates for use in the development of buoyant swimwear. For the mechanical properties, EPEnH3 is more difficult to compress than EPEn3. This shows that EPEnH3 may retain a higher buoyancy under the same load of compression when used for swimwear. For the tensile properties, EPEn3 is more stiff than EPEnH3 under elongation in the wale direction, which may reduce the comfort of the swimwear during swimming. EPEnH3 shows better specific buoyancy, compression and tensile properties than EPEn3.

Further Research

Two approaches were used to incorporate buoyant materials into knitted fabric, including knitting the buoyant materials by treating them as a knitting yarn (Approach 1) or inlaying the buoyant material into the fabric during knitting (Approach 2, which was reported in this MOC).

In Approach 1 (Figure 20), only silicone foam could be spun into a corded yarn, with PP as the cover layer. However, the resultant corded yarn was approximately 7 mm thick, which is too thick for use as a knitting or inlay material. The weight of the yarn increased after spinning because the outer layer of PP was thick compared with the fine core foam (a). In the fancy twisting process, the thread could not be evenly twisted onto the foam rod because the silicone foam has high stretchability. Some parts of the rod had large buds of thread, and other parts had no threads twisted onto them (b). The thread on the rod was loose, which might have caused the entanglement of the threads in the needle beds during the knitting process. As such, the knitting process could not proceed further because doing so would damage the knitting machine. Therefore, the aforementioned methods are impractical for modifying the buoyant tube/rods. In the future, the research team should invest more time and effort in examining this approach in order to provide data for comparison with the buoyant performance in the present study.

Figure 20. Yarn treatment after (a) spinning and (b) fancy twisting

Research Dissemination

Academic Journal Articles

Li, N. W., Ho, C. P., Yick, K. L., & Zhou, J. Y. (2022). Development of laid-in knitted fabric for buoyant swimwear. Journal of Industrial Textiles, 51(9), 1397-1411. (https://doi.org/10.1177/1528083719900932)

Li, N. W., Ho, C. P., Yick, K. L., & Zhou, J. Y. (2021). Influence of inlaid material, yarn and knitted structure on the net buoyant force and mechanical properties of inlaid knitted fabric for buoyant swimwear. Textile Research Journal, 91(13-14), 1452-1466. (https://doi.org/10.1177/0040517520981742)

Exhibition Poster Presentation

School of Design, The Hong Kong Polytechnic University (May 2025)

References

Cai, K., Pritikin, E., Sandland, N., & Charno, L. (2011). Achieve PVC properties in new medical TPE compounds-Novel TPE compounds achieve high levels of performance and acceptance due to an approach that focuses on functional attributes rather than generating laboratory data. Rubber World, 244(3), 18.

Chong, H. K., Kan, C. W., Ng, S. P., & Hu, H. (2013). Study on the relationship between UV protection and knitted fabric structure. Journal of Textile Engineering, 59(4), 71-74.

Cole-Hamilton, D. J. (2010). Nature's polyethylene. Angewandte Chemie International Edition, 49(46), 8564-8566.

Gadler NN. Body surfing suit. Patent 8,662,946, U.S., 2014

Gagnon, D., McDonald, G. K., Pretorius, T., & Giesbrecht, G. G. (2012). Clothing buoyancy and underwater horizontal swim distance after exiting a submersed vehicle simulator. Aviation, Space, and Environmental Medicine, 83(11), 1077-1083. doi:10.3357/ASEM.2933.2012

Kalayci, E., Yildirim, F. F., Avinc, O. O., & Yavaş, A. Textile fibers used in products floating on the water. In: 7th International Scientific Professional Conference: Textile Science and Economy VI, Zrenjanin, Serbia, 25–31 May 2015, pp. 85–90. University of Novi Sad, Technical Faculty.

Kiriktaş, H., Şahin, M., Eslek, S., & Kiriktaş, İ. (2018). A new approach to determine the density of liquids and solids without measuring mass and volume: introducing the solidensimeter. Physics Education, 53(3), 035009.

References

Lee, S. H. (2017). U.S. Patent No. 15/303739. Washington, DC: U.S. Patent and Trademark Office.

Lu, S., Duan, ., Han, Y., & Huang, H. (2013). Silicone rubber/polyvinylpyrrolidone microfibers produced by coaxial electrospinning. Journal of Applied Polymer Science, 128(4), 2273-2276.

Nelson, M. R., Krapp, K. M., & Gale, G. Density and Buoyancy. Experiment Central Understanding Scientific Principles Through Projects. 2nd ed. Detroit: U--L, 2010, pp. 257–260.

Staver, B. J., & Vaughn, N. (2008). U.S. Patent No. 7,438,619. Washington, DC: U.S. Patent and Trademark Office.

Shaffer, C. K. (2000). U.S. Patent No. 6,112,327. Washington, DC: U.S Patent and Trademark Office.

Zhang, Y. H., Kan, C. W., & Lam, K. C. (2015). A study on ultraviolet protection properties of 100% cotton knit fabric: effect of fabric structure. The Journal of the Textile Institute, 106(6), 648-654. doi:10.1080/00405000.2014.933514